Sensing and Bio-Sensing Research 34 (2021) 100458

Contents lists available at ScienceDirect

Sensing and Bio-Sensing Research

journal homepage: www.elsevier.com/locate/sbsr

Microfluidic system evaluation for the semi-automatic detection of MOG-IgG in serum samples

Numfon Khemthongcharoen [a], Panapat Uawithya [b], Nutthapon Yookong [b], Mayuree Chanasakulniyom [c], Wutthinan Jeamsaksiri [d], Witsaroot Sripumkhai [d], Pattaraluck Pattamang [d], Ekachai Juntasaro [e], Nongluck Houngkamhang [f], Therdthai Thienthong [e], Chamras Promptmas [a,*]

[a] Department of Biomedical Engineering, Faculty of Engineering, Mahidol University, Nakhon Pathom, Thailand
[b] Department of Physiology, Faculty of Medicine, Siriraj Hospital, Mahidol University, Bangkok, Thailand
[c] Department of Clinical Chemistry, Faculty of Medical Technology, Mahidol University, Bangkok, Thailand
[d] Thai Microelectronics Center (TMEC), NECTEC, National Science and Technology Development Agency (NSTDA), Thailand
[e] Mechanical Engineering Simulation and Design Group, The Sirindhorn International Thai-German Graduate School of Engineering (TGGS), King Mongkut's University of Technology North Bangkok (KMUTNB), Bangkok, Thailand
[f] College of Materials Innovation and Technology, King Mongkut's Institute of Technology Ladkrabang, Bangkok, Thailand

ARTICLE INFO

Keywords:
Cell culture microfluidics
Myelin oligodendrocyte glycoprotein reactive immunoglobulin G antibody (MOG-IgG)
Serial dilution microfluidics
Microfluidic cell-based immunofluorescence assay

ABSTRACT

Myelin oligodendrocyte glycoprotein reactive immunoglobulin G antibody (MOG-IgG) is in patients with central nervous system demyelination. Reliability of the conventional detection method relies on technician skills and pipetting error accumulation. This work develops a microfluidic system for semi-automatic MOG-IgG detection using cell-based immunofluorescence (IF) assay. The polydimethylsiloxane (PDMS) microfluidic was modified by poly-L-lysine to enhance the adhesion of Human embryonic kidney (HEK) cell. The untransfected and GFP-MOG transfected HEK cells were cultured, fixed, and stained in the microfluidic with the feeding reagents regulated by a syringe pump. Cell characterization, limit of detection (LOD), and turnaround time of the IF assay operation in microfluidic were compared to those in standard microplate. In microfluidic, cell-clumping formation can be avoided and thus signal variations that are caused by cell overlapping can be significantly reduced. LOD of MOG-IgG detection in the microfluidic is at least 2.5 times better than that in the microplate. Signal intensities of the IF staining for 1 h in microfluidic are comparable to those stained for overnight in the standard microplate. By integration with a serial dilution microfluidic, the optimal cutoff titer for MOG-IgG positivity in the patient samples was determined by Receiver operating characteristic curve (ROC) analysis.

1. Introduction

Myelin oligodendrocyte glycoprotein reactive immunoglobulin G (MOG-IgG) is a serological autoantibody that has been found in patients who have autoimmune disease related with CNS demyelination such as Neuromyelitis Optica Spectrum Disorder (NMOSD), myelitis, cortical encephalitis, and acute disseminated encephalomyelitis [1–3]. Clinical features of MOG antibody disorder (MOG-AD) are similar to many CNS inflammatory related disorders especially in NMOSD [4,5]. However different patterns of the serological MOG-IgG positivity are disparate in some clinical symptom characterization and prognosis of the disease [6–9]. Investigations of serological AQP4-IgG and MOG-IgG are thus required for differential diagnosis and individual treatment planning in the patients.

Laboratory techniques for MOG-IgG detection consists of tissue-based immunoassay [10,11], ELISA [12], western blot (WB) [13], radio immunoprecipitation assay [14], and cell-based assay (CBA) [15,16]. Tissue-based assay encounters the problems of MOG antigen quantity control and the resource consuming in the tissue sample preparation process. Both ELISA and WB techniques lack of dependability to define MOG-IgG distinction in CNS demyelination related disorders [17,18]. Because the immunological interaction of MOG-IgG is

* Corresponding author at: Department of Biomedical Engineering, Faculty of Engineering, Mahidol University, 999 Phutthamonthon 4 Road, Salaya, Nakhon Pathom 73170, Thailand.
E-mail address: chamras.pro@mahidol.ac.th (C. Promptmas).

https://doi.org/10.1016/j.sbsr.2021.100458
Received 16 April 2021; Received in revised form 27 September 2021; Accepted 4 October 2021
Available online 6 October 2021

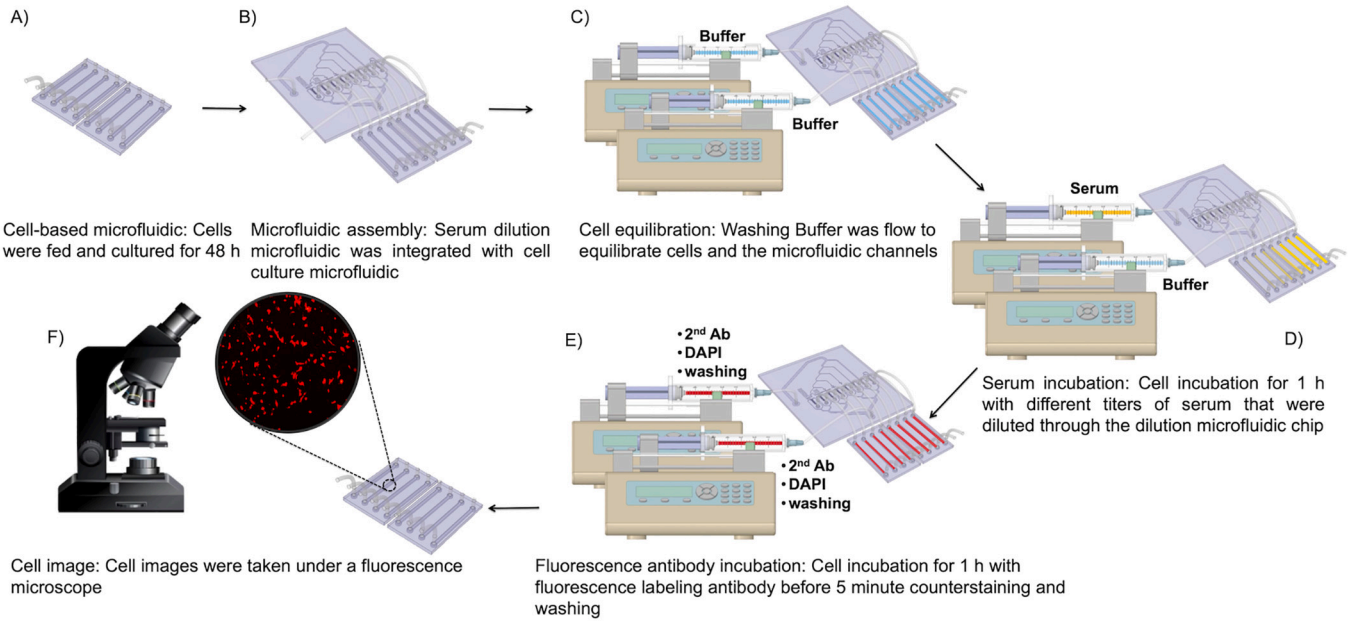

Fig. 1. A schematic demonstrates the step protocol for the serological examination of MOG-IgG in patient serum. A cell-based microfluidic with HEK cell fixing (A) was assembled with a serum dilution microfluidic (B). Both inlets of the dilution microfluidic were connected with syringe pumps to feed the equilibrating buffer (C). Serum sample and dilution buffer were fed via the serum and buffer inlets to prepare different titers of the serum sample (D). Then the cells were sequentially stained with Alexa Fluor 555-conjugated human IgG, DAPI counterstain before washing with PBS (E). The stained cells in the microfluidic were observed under a fluorescence microscope (F).

strictly conformational dependent, ELISA and WB techniques that apply either liner peptide detection or denatured MOG protein as the immunological target fail to recognize pathogenic MOG-IgG [1,19]. Cell-based assay (CBA) employs full-length human MOG expressing cell for the immunostaining assay, in which posttranslational modification and conformation of MOG protein can be preserved similarly to native MOG protein. Thus, sensitivity and specificity for the detection of pathogenic MOG-IgG are better than WB and ELISA-based techniques. The CBA-based technique has been used either in fixed cell-based immunofluorescence (IF) test or in live flow cytometry (fluorescence-activated cell sorting [FACS]) test. Both IFT and FACS tests are currently recommended as the gold standard method for MOG-IgG detection [12]. The previous research demonstrated that live FACS-CBA technique provided good correlative results among the international multicenter examination [18]. However live FACS-CBA technique is difficult to be operated in clinical laboratory because the technique requires extensive cell culture infrastructure for live cell preparation. The test also has to be conducted in an expensive flow cytometer by a skilled technician. Fixed cell based IF test in which the cells can be prior fixed in the microplate is more practical for clinical laboratory operation. However, Staining quality and reproducibility of the technique are depended on technician skills and are relied on manual pipetting errors. Positivity of the cell is examined by visual observation under a fluorescence microscope. Thus, reliability of the result is also based on subjective experiences of the medical staffs. The optimal cutoff titers of MOG-IgG to classify group of CNS demyelinating patients are also different depending on the diagnosis platform [12,18,20,21].

This work develops a cell-based microfluidic system for serological MOG-IgG detection. IF assay operation in microfluidic consumes ultimate low volumes of both sample and reagents. Method variations and contamination risk can be avoided by integration of the microfluidic with an accurate liquid flow regulator. Combining with image analysis program, positivity of the IF-stained cells can be determined based on measurable fluorescence signal intensity. An optimal cutoff titer was determined by Receiver operating characteristic curve (ROC) analysis using 20 patient samples, which were previously examined for MOG-IgG positivity by an external reference laboratory. The samples were fed through a serial dilution microfluidic chip, in which 8 different serum titers can be evaluated simultaneously.

2. Material and methods

2.1. Cell-based microfluidic preparation

The microfluidics were fabricated by mixing polydimethylsiloxane (PDMS) prepolymer and curing agent (DOW CORNING *Co*., Midland, U.S.A.) at 10:1 ratio. The mixer was casted on a silicon wafer with 1500 × 30,000 × 50 μm in width × length × depth microchannel pattern. Then, the prepolymer was degassed and solidified at 75 °C for 2 h. PDMS microchannel was bonded on flat PDMS sheet by oxygen plasma treatment at 30 watts RF power for 150 s. The microfluidic chip was baked at 95 °C for 3 min then inlet and outlet tubes were lined. The microfluidic channels were immediately incubated with 0.01% poly-L-lysine (PLL) (SIGMA-ALDRICH *Co*., *St*. Louis, U.S.A.) for at least overnight. The modified microfluidic chips were kept at 4 °C until use. Before cell seeding, the microfluidics were washed with 200 μl phosphate buffer saline (PBS) pH 7.4 (MERCK, Darmstadt, Germany). The suspensions of untransfected and GFP-MOG transfected HEK cells at 3–5 × 10^6 cells/ml in Dulbecco's Modified Eagle Medium (DMEM) (GIBCO, New York, U.S.A.) with 10% fetal bovine serum (FBS) (SIGMA-ALDRICH *Co*., *St*. Louis, U.S.A.) supplementation were filled in the PLL modified microfluidics. Cells in the microfluidics were incubated for 48 h in moist chamber at 37 °C with 5% CO_2. Cell adhesion in microfluidic chip was observed under a phase contrast microscope. The behavior of HEK cells suspended in the multiphase flow inside the microfluidic chip was simulated by using the commercial CFD software ANSYS FLUENT 2020R2 [ANSYS 2020]. The Discrete Phase Model (DPM) was used to predict the HEK-cell distribution in a Lagrangian reference frame. The input parameters for simulation were the DMEM density of 10% FBS at 1.009 g/cm^3 [22], the average HEK-cell diameter of 10–15 μm [23,24], and the HEK-cell wet weight of 2.55 ng [25]. The channel had one inlet and one outlet with the same circular diameter of 500 μm. Only half of the channel

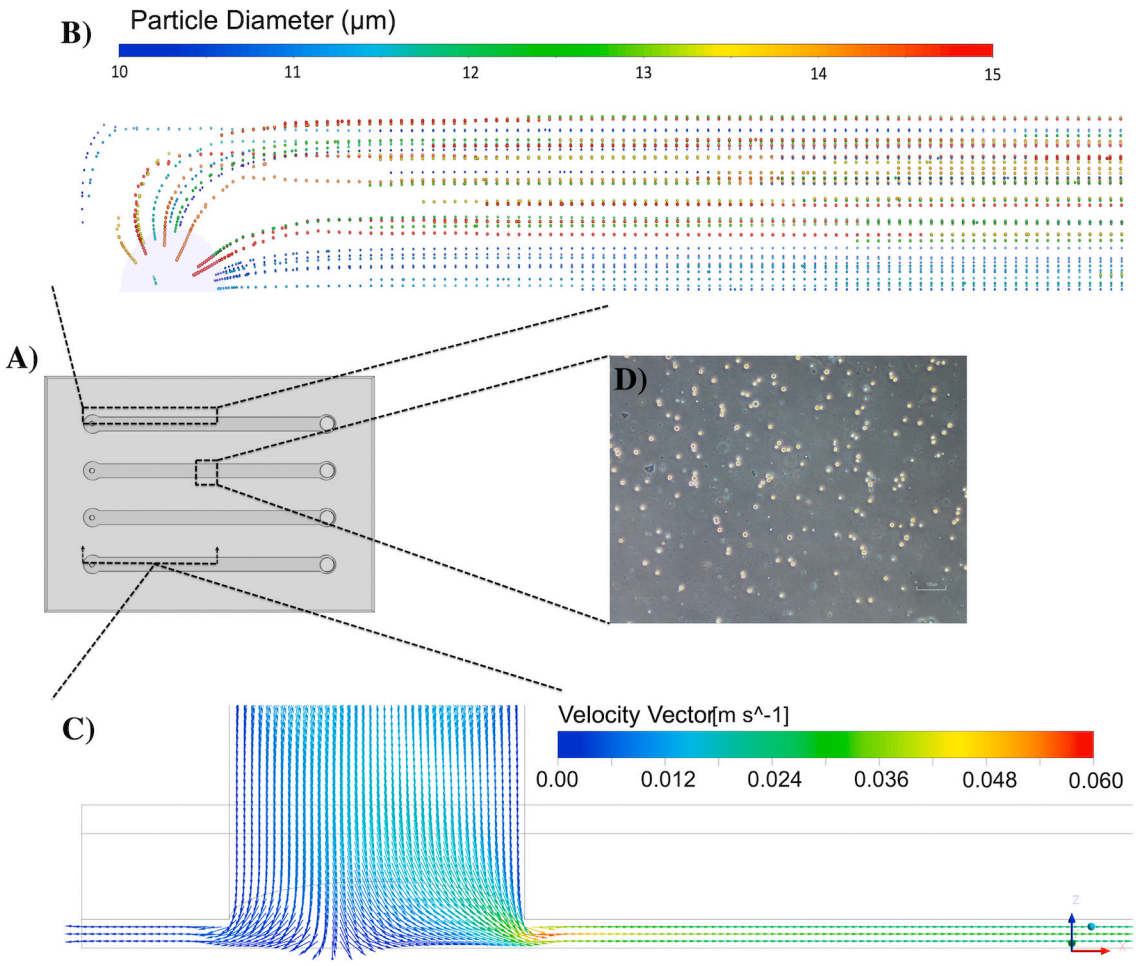

Fig. 2. Simulation of the cell flow in one-fourth of each microfluidic channel in the microfluidic chip (A). Top view of the cell flow tracks indicating HEK cell distribution after feeding through the inlet (B). Velocity vector of the cell flow revealing the flow pattern in the microfluidic chip (C). Microscopic image demonstrating the distribution of HEK cells in the microfluidic chip (D).

domain was considered because the fluid domain was symmetrical with respect to the symmetry plane, which was located in the middle of the channel width as shown in Fig. 1.

2.2. Cell-based IFT performing in the microfluidic

Before the IF staining process, the untransfected and GFP-MOG transfected HEK cells in the microfluidics were washed for 15 min by PBS. Then the cells were fixed with 4% paraformaldehyde for 30 min, washed with 0.1% tween 20 (USB *Co*. Cleveland, U.S.A.) in PBS buffer, permeabilized with 0.5% triton X-100 (USB *Co*. Cleveland, U.S.A.) in PBS buffer for 30 min, and washed with PBS buffer for 15 min. The cells were incubated with 5% bovine serum albumin (BSA) in 0.1% tween 20 (USB *Co*. Cleveland, U.S.A.) in PBS for at least 1 h to block non-specific antibody binding. The cells were stained with either rabbit anti-human MOG IgG (SINO BIOLOGICAL, Pennsylvania, U.S.A.) for method evaluation or with patient sera for ROC curve analysis. The cells were washed for 15 min and stained with Alexa Fluor 555 conjugated antibody to detect either rabbit IgG or human IgG (Life Technologies, New York, U.S.A.) regarding to the primary antibody used in the previous step. Nucleus of the cells were stained for 5 min with 1 μg/ml 4′,6-Diamidino-2-Phenylindole, Dihydrochloride (DAPI) (Life Technologies, New York, U.S.A.) and washed with PBS buffer for 15 min. All reagents were sequentially fed into the microfluidic channel at a constant flow rate of 20 μl/min by a multichannel syringe pump regulation. Each microfluidic channel was filled with glycerol before collecting the fluorescence images under a fluorescence microscope at 100× magnification. Fluorescence images of the cells in each field of view were captured via blue, green and red filter cubes of the fluorescence microscope.

2.3. Standard cell-based IFT in 96-well microplate

The untransfected and GFP-MOG transfected HEK cells at approximate 6000 cells were seeded into each well of a black microtiterplate. The cells were grown for 48 h in 37 °C with 5% CO_2 supplementation. Cells in each well were washed, fixed, blocked, and stained with the sequence of solutions as previously described in the staining protocol used in the microfluidic platform. Cell images in each well were collected under a fluorescence microscope at 100× magnifications by blue and red filter cubes of the fluorescence microscope. Fluorescence signal of on each cell was individually analyzed by utilizing the fluorescence image analysis protocol as described below.

2.4. Immunoserological assay examination

The cell-based microfluidic was further evaluated with the patient serum samples, which its MOG-IgG positivity results were previously examined using the reference method by an external laboratory. The cell-culture microfluidic was assembled to a serum dilution microfluidic

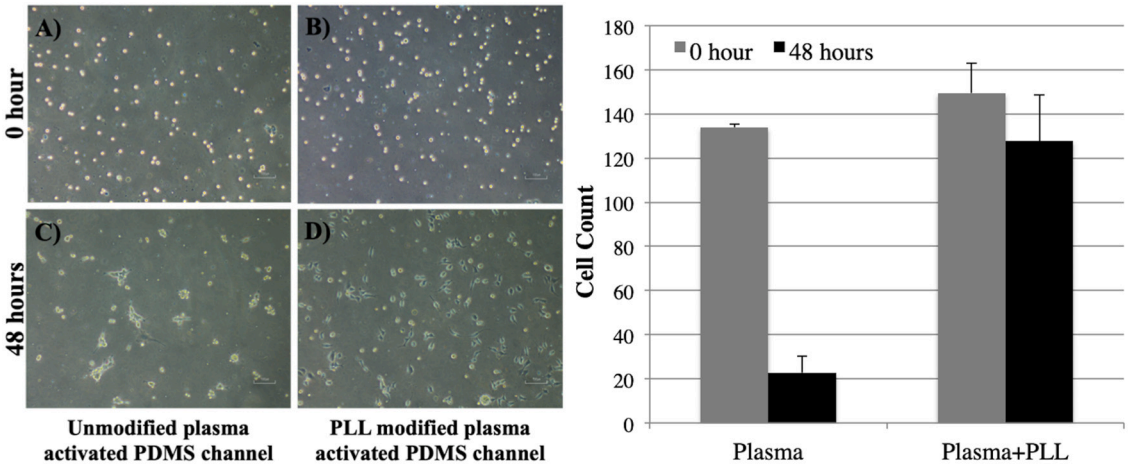

Fig. 3. Adhesion efficacy of HEK cell in oxygen plasma activated microfluidics with and without PLL modification at 0 ^{h} (A and B) and after 48 ^{h} (C and D) incubation. Average number of HEK cell per field of view in oxygen plasma activated microfluidic with and without PLL modification (E) at 0 ^{h} (gray bar) and after 48 ^{h} (black bar) incubation ($n = 5$).

chip. After 15 min of cell equilibration by 5% BSA in 0.1% tween 20 in PBS (equilibrating buffer), a serum sample and the dilution buffer were flowed through the dilution microfluidic chip as the schematic procedure shown in Fig. 1. In the dilution microfluidic chip, different proportions of the microfluidic channels were designed to generate different titers of the serum sample. The serum sample and the dilution buffer were mixed together by a serpentine microfluidic structure as the details described in our previous work [26]. HEK cells fixed in the cell culture microfluidic were incubated with different titers of the serum sample for 1 h. Then the cells were washed and sequentially stained as described previously described in 2.2. The cell culture microfluidic was disassembled from the dilution microfluidic. Fluorescence images of the cells that were stained in each microfluidic channel were collected under a fluorescence microscope at 100× magnification.

2.5. Fluorescence image analysis

Locations of the individual cell were observed from DAPI nuclear staining. Each of cells was arbitrarily cropped to obtain at least 200 cells per sample. Mean fluorescence intensity (MFI) of every pixel in each cell was determined regarding to their grayscale level (8-bit grayscale image; black (0) – white (225)). MFIs of green and red signals were measured by ImageJ 1.44 image analyzer program [27]. Green and red MFIs of the individual cell indicate the success of GFP-MOG transfection and MOG-IgG IF staining, respectively.

2.6. Plasmid construction and GFP-MOG expression in HEK293T cell

pSF-MOG-daGFP plasmid was constructed by PCR amplification of pMD18-T-simple containing human MOG transcript variant 1 (HG10364-M) (Sinobiological Inc., China) using 5′-AGGAGGTACC-CACCATGATGGCAAGCTTATCAAGA-3′ forward primer and 5′- GAG-GAGACAACTTCTATCAGAAGGGATTTCGTAGCT-3′ reverse primer. The construction plasmid was transfected into HEK293T cell by using Lipofectamine® 3000 reagent. The transfected cell was cultured in DMEM medium supplemented with 10% FBS under the optimal cell culture condition.

2.7. Serum samples

Negative control sample is a pool of the leftover sera collected from at least 50 healthy blood donors who attended their blood donation at department of transfusion medicine, Siriraj hospital. Clinical serum samples using in this study were collected from patients who attended to neurology clinic, Siriraj hospital. All sample collections were conducted by an appropriate sample management protocol approval from Siriraj Institutional Review Board (approval number SI 330/2016).

2.8. Statistical analysis

Statistical analysis was conducted by SPSS software. Between-group comparison of average MFIs obtained from the untransfected and GFP-MOG transfected HEK cells were analyzed by Mann-Whitney *U* test. The microfluidic system was evaluated with 20 clinical samples that were previously examined by an external laboratory using standard reference method. ROC curve that is a plot between sensitivity versus 1-specificty (false positive rate) of 20 serum sample evaluations in the microfluidic comparing to those evaluated by the standard reference method was conducted using the result agreement at 95% confidence interval (CI). ROC curves of the serological examination by using different serum titers were analyzed to find the titer that offers the best sensitivity and specificity (the highest area under the ROC curve) for serological MOG-IgG detection in the microfluidic platform.

3. Results

3.1. Cell-based microfluidic preparation

For the cell-seeding step, all microfluidic channels were filled with HEK cells suspended in the microfluidic chip as shown in Fig. 2 (A). The simulation result of the cell flow is demonstrated in Fig. 2 (B) and (C). Fig. 2 (B) reveals the cell flow tracking simulation in one-fourth of a microfluidic channel. The result indicates that HEK cells, whose diameters are 10–15 μm [23,24], can be spread throughout the microfluidic substrate. The velocity vector plot in Fig. 2 (C) demonstrates the flow pattern of HEK cells suspended in the microfluidic channel. With this flow pattern in Fig. 2 (C), the HEK cells are forced to flow orderly in multilayers above the substrate surface where the maximum velocity is in the middle of the channel (half height of the channel). The HEK cells with the maximum velocity are forced to flow out from the microfluidic channel but, as the flow velocity decreases toward the substrate surface and becomes zero at the substrate surface, the HEK cells in the lowest layer (at about 8 μm) adjacent to the substrate surface are stagnant and eventually stick to the substrate surface. Fig. 2 (D) reveals the HEK cells remaining on the substrate surface in the microfluidic chip that were observed under a 100× phase contrast microscope. The microscopic image confirms the single layer of HEK cells spreading over the microfluidic surface.

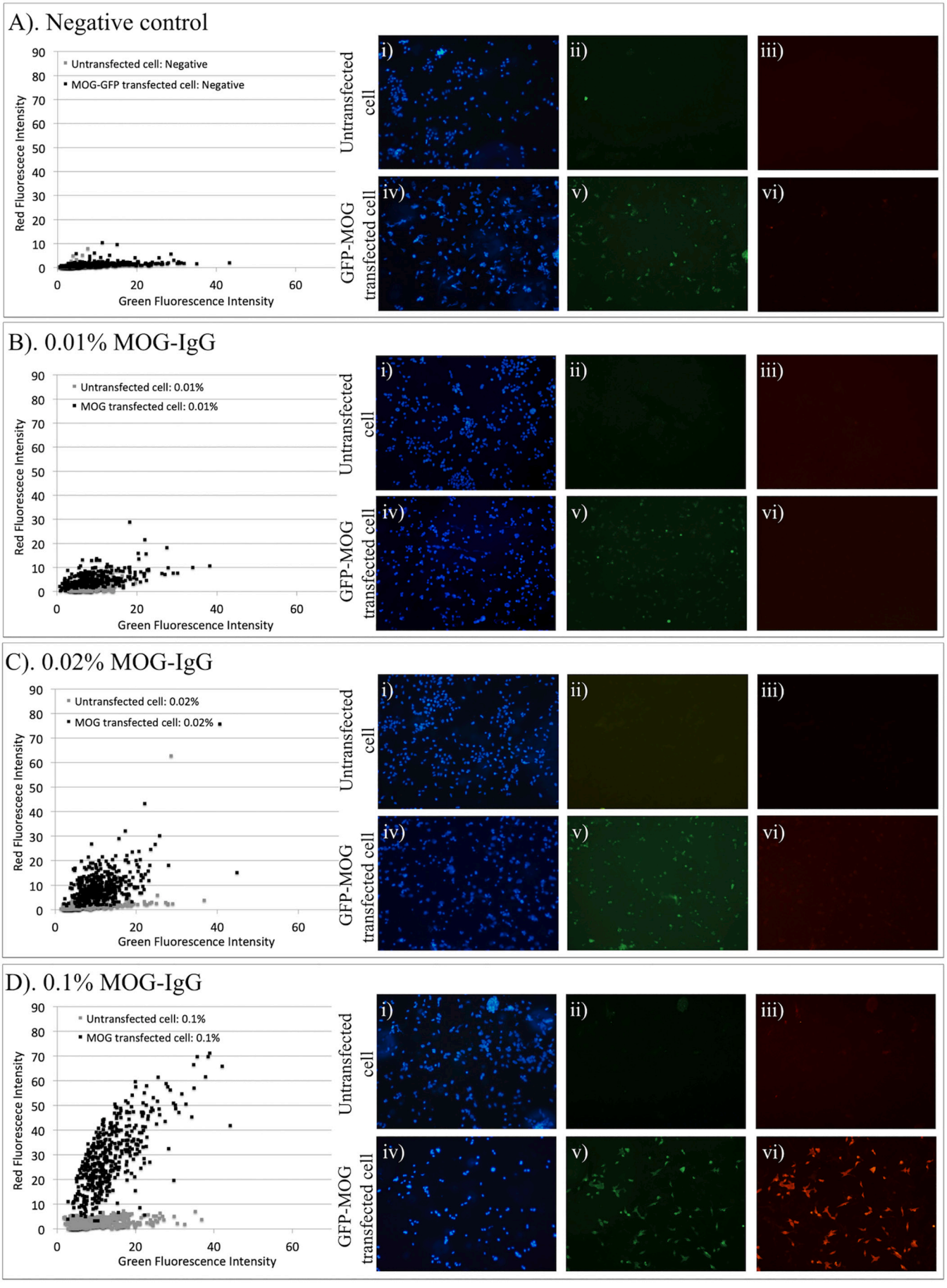

(caption on next page)

Fig. 4. Relative correlation plots of green against red MFIs on the untransfected HEK cells (gray dot) and GFP-MOG transfected (black dot) HEK cells that were stained by 0 (A), 0.01 (B), 0.02 (C), and 0.1 (D) % *V*/V of rabbit anti-Human MOG in the dilution buffer. Examples of blue, green, and red fluorescence images of the untransfected (i, ii, and iii) and GFP-MOG transfected cells (iv, v, and vi) that were stained by each of rabbit anti-Human MOG concentrations. (For interpretation of the references to colour in this figure legend, the reader is referred to the web version of this article.)

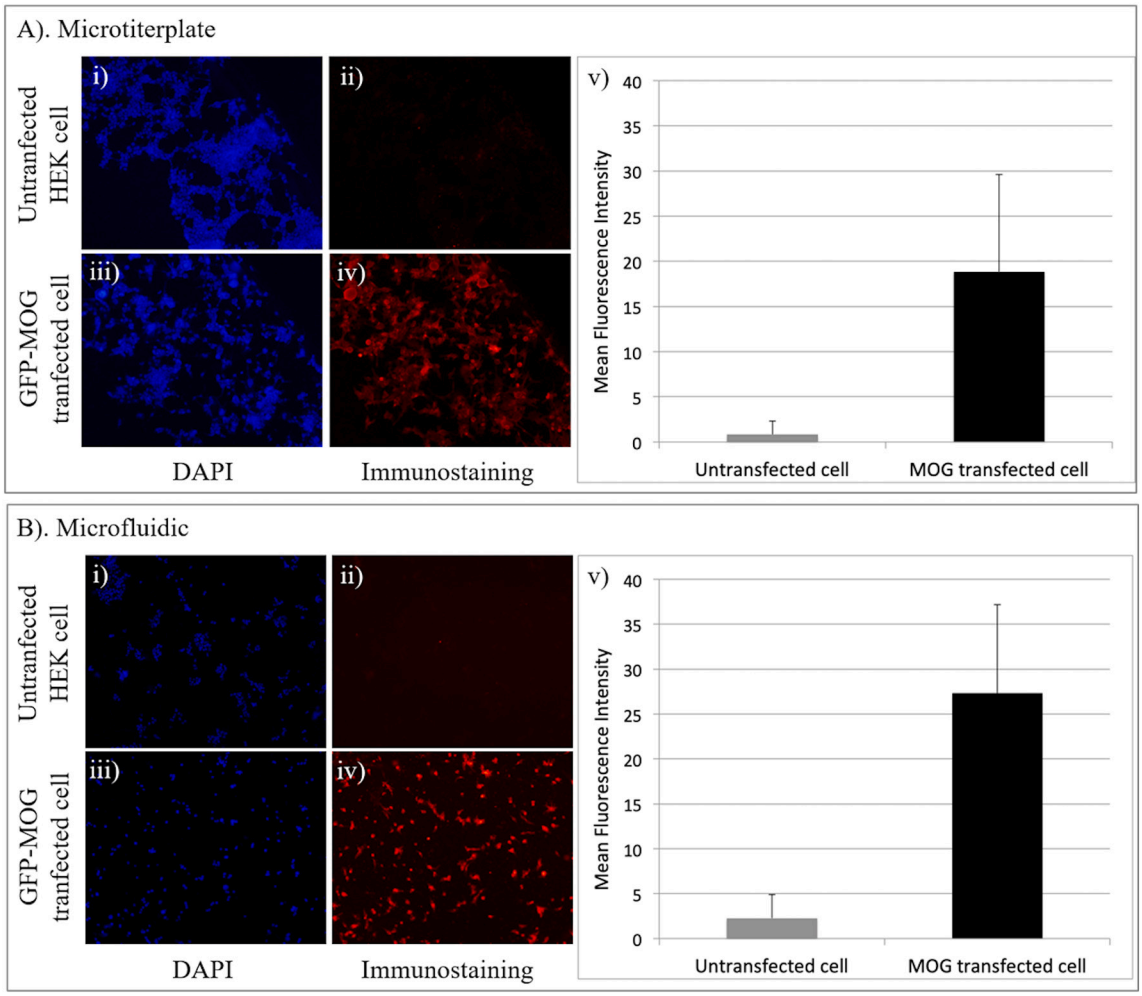

Fig. 5. IF images and average IF signal obtained from the untransfected and GFP-MOG transfected HEK cells in standard microplate (Upper) and in microfluidic (Lower). The fluorescence images showing the blue signal of DAPI nuclear staining and the red IF signal of MOG-IgG IF staining on the untransfected (i and ii), and on GFP-MOG transfected cells (iii and iv), and average IF signals of both (v) cells in microplate and in microfluidic. (For interpretation of the references to colour in this figure legend, the reader is referred to the web version of this article.)

Due to inherit hydrophobicity of PDMS, the microfluidic was modified by PLL to enhance the adhesion of HEK cell. Fig. 3 shows the adhesion of HEK cells in the oxygen plasma activated microfluidic channels with and without PLL modification. Oxygen plasma activated microfluidics with and without PLL modification were filled with 3×10^6 cell/ml HEK cell suspension. Immediately after cell seeding, average numbers of the cell per field of view (FOV) in the microfluidics with and without PLL modification are not significantly different. However, average number of the attached HEK cells after 48 ^{h} incubation in PLL modified microfluidic is 5 times higher than those attached in the microfluidic without PLL modification. The result indicates that the oxygen plasma activated PDMS with PLL modification significantly improve the HEK cell adhesion in the PDMS microfluidic channel.

3.2. Correlation between GFP-MOG protein expression and IF staining signal

The cells in PDMS microfluidic were stained for 1 ^{h} by various concentrations of rabbit anti-Human MOG solution. After IF staining, the cells were individually measured for their green and red MFIs using imageJ program. Green and red fluorescence signals indicate the success of GFP-MOG expression and MOG-IgG staining efficacy on each cell, respectively. The relative plots in Fig. 4 show the correlative increase of red and green MFIs. These results indicate positive correlation between GFP-MOG protein expression and immunofluorescence staining efficacy on each cell. Average green MFIs of GFP-MOG transfected cells are significantly higher than those of the untransfected cells. Average red MFIs of negative control, 0.01%, 0.02%, and 0.1% rabbit anti-Human MOG solutions staining on the GFP-MOG transfected cells are 0.6040 (95%CI [0.5069, 0.7011]), 4.0381 (95%CI [3.7016, 4.3745]), 7.6807 (95%CI [7.0696, 8.2918]), and 26.6787 (95%CI [25.4403, 27.9171]) higher than those staining on the untransfected cells. Results in this study demonstrate the successfulness of GFP-MOG transfection and MOG-IgG IF staining on the transfected cell in the microfluidic platform.

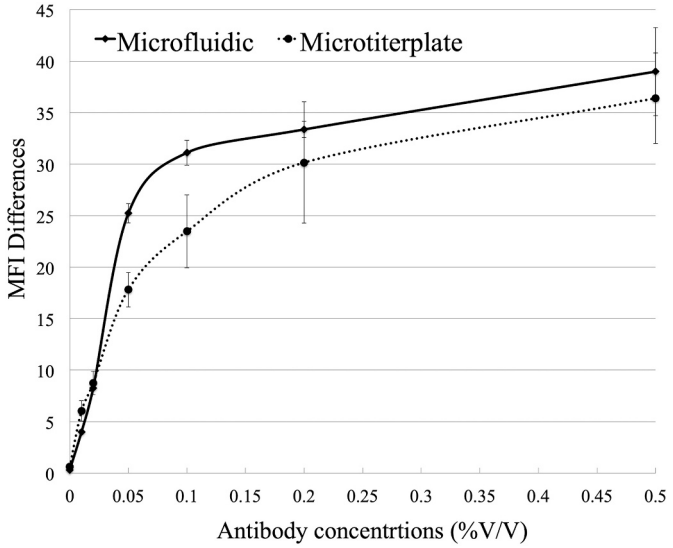

Fig. 6. The IF signal differences between the untransfected and GFP-MOG transfected HEK cells that were stained by different MOG-IgG concentrations varying from 0 (Negative) to 0.5%V/V rabbit anti-human MOG IgG in standard microplate (dashed line) and in microfluidic channel (solid line).

3.3. Cell distribution in the culture vessels

Fig. 5 demonstrates IF images of the cells that were stained by 0.5% rabbit anti-Human MOG in standard microplate for overnight and in microfluidic channel for 1 h.

The fluorescence images show that cell clumping formations can be found in standard microplate particularly at the edge of the microplate. The cells are well distributed in the microfluidic. Adequate cell distribution in microfluidic can be a further benefit to the image processing protocol, in which cell overlapping causing an accumulative error of the signal collection can be avoided. Average MFIs as shown in Fig. 5; A5 and B5 obviously indicate that IF signals on GFP-MOG transfected cell are significantly higher than that on the untransfected cells. The average MFI of GFP-MOG transfected cells that were stained for 1 h in microfluidic are comparable to that of the cells that were stained for overnight in standard microplate.

3.4. Limit of detection of the IF assay

The untransfected and GFP-MOG transfected HEK cells were stained by rabbit anti-human MOG IgG at 0, 0.01, 0.02, 0.05, 0.1, 0.2, and 0.5% (*V*/V) in for overnight in microplate and for 1 ^{h} in microfluidic. After sequential IF staining process, MFI of red fluorescence signal on each cell was measured by ImageJ program. The differences between average MFIs of the untransfected and MOG-GFP transfected HEK cells are shown in Fig. 6. The differentiated signals in the microfluidic are obviously higher than those in the microplate. In microfluidic, the signal difference rapidly increases with the IgG concentration until reaching the saturated level at 0.2% (*V*/V). Limit of detection (LOD) of the cell staining in each platform was estimated as described previously in 2008 by Armbruster and Pry [28]. LODs for MOG IgG investigation in microplate and in microfluidic are, 2.56 and 0.94, respectively. This experiment confirms that microfluidic platform obviously improves LOD of the cell-based IF assay for MOG-IgG detection.

3.5. Effect of incubation period on the IF staining efficacy

Cells in standard microplate and in microfluidic channel were stained with 0.05% rabbit MOG-IgG and anti-rabbit IgG by the incubation periods varying from 15 to 60 min. The immunostaining results are

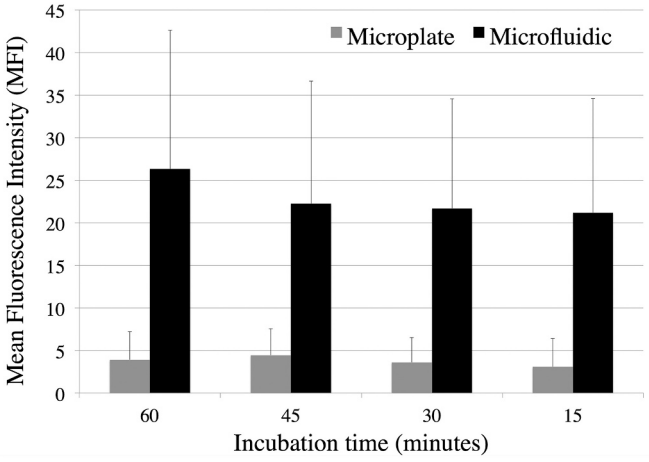

Fig. 7. Average MFI differences between the untransfected and GFP-MOG transfected HEK cells that were stained in standard microplate (gray bars) and in the microfluidic (black bars) by using the incubating period varying from at 15 to 60 ^{min}.

demonstrated in Fig. 7. For all incubation periods, the differentiated signals that were performed in the microfluidic are obviously better than the signals from microplate. In microfluidic platform, the incubation period can be reduced to 15 min with only approximated 5% differentiated signal reduction. This result demonstrates advantages of the liquid flow phenomenon in microfluidic that can improve turnaround time of the cell based IF assay.

3.6. Clinical sample test and receiver operating characteristic curve (ROC) analysis

The cell-based microfluidic platform was evaluated with 20 patient serum samples. Negative control sample was collected from at least 50 healthy blood donors. Serum samples of the patients were screened at 1:4 on the GFP-MOG transfected HEK cells fixed in the microfluidic channel. The samples that reveal positive signal at 1:4 titer over the signal obtained from the negative control sample staining were further evaluated for an optimal cutoff dilution by using ROC analysis. Each serum sample at the titer of 1:4 was flowed through a 2-fold serial dilution microfluidic chip connected to the cell-culture microfluidic channel as demonstrated in Fig. 8. The serum sample and the dilution buffer were mixed in the microfluidic serpentine structure that were previously optimized and evaluated in our previous work [26]. Serum sample and the dilution buffer were fed into the sample inlet and the buffer inlet of the serial dilution microfluidic to generate 8 sample titers. Thus, the untransfected and GFP-MOG transfected cells in each cell-culture microfluidic channel were stained by different titers of the sample varying from 1:4–1:256. Average MFIs of GFP-MOG stained cells in each of the cell-culture microfluidic channels were subtracted by average MFIs of the untransfected HEK cell stained by the same sample titer. The sample titers at 1:4 and 1:8 equally reveal the maximum area under ROC curve, which is 0.957. This result indicates that the sample titers at 1:4 and 1:8 are the optimal cutoff titers that offer the best sensitivity and specificity for serological MOG-IgG detection in the microfluidic platform using the serological examination by standard cell-based immunoassay as a reference method.

4. Discussion

PDMS is one of the most well known polymers that have been widely used for microfluidic fabrication [29]. However, its inherit hydrophobicity has to be modified to inhibit non-specific adsorption of proteins and to enhance attachment of the cell [30,31]. The functionalization

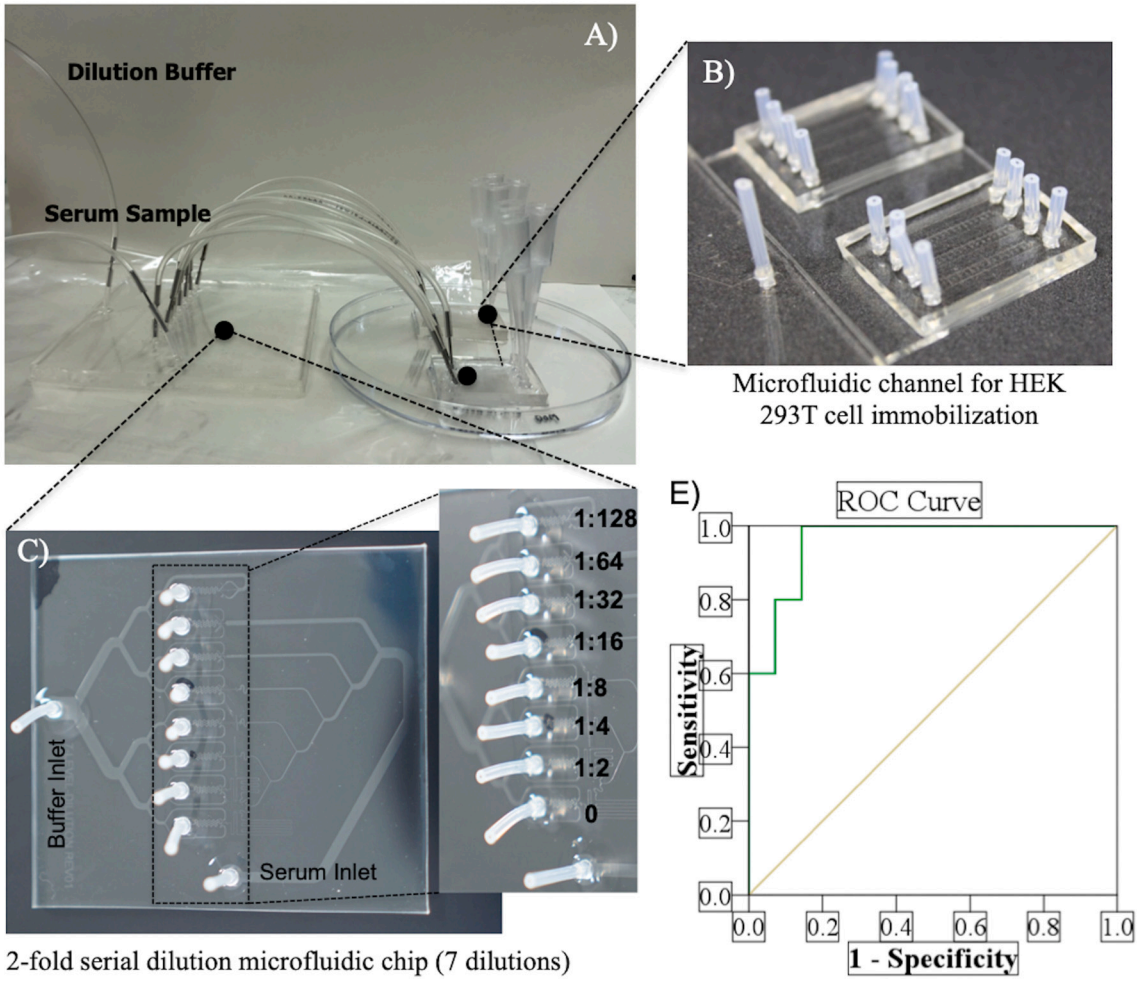

Fig. 8. The microfluidic system (A) consisted of the cell-based microfluidic chips (B) a serial dilution microfluidic chip that provides 2-fold serial dilutions of serum sample varying from 1:2 to 1:128 titers (C). ROC curve of MOG-IgG examination in 20 serum samples at 1:4 and 1:8 titers evaluated by the microfluidic platform compared to the results from reference method examined by an external laboratory using the result agreement at 95% CI (D).

materials that have usually been applied to modify the hydrophilicity of PDMS are consisted of extracellular matrix components, hydrophilic polymers, and non-ionic surfactants [32–35]. In our previous study, we compared efficiency of the PDMS microfluidic modified either by an extracellular matrix (poly-L-lysine; PLL), a hydrophilic polymer (polyvinyl alcohol; PVA) or a non- ionic surfactant (pluronic F127) to enhance surface hydrophilicity and the adhesion of HEK cell. We found that PLL modification obviously promotes the adhesion of HEK cell even though the hydrophilicity of PLL modified PDMS did not significantly differ from that of the unmodified PDMS [36]. The untransfected and GFP-MOG transfected HEK cells were cultured in the PLL modified PDMS microfluidics to prepare the cell-based microfluidic chip for serological MOG-IgG examination.

Basic advantages of the microfluidic application in the field biomedical diagnosis are ultimate reduction of reagents and sample consuming, affordable mass production, available for an automatic flow regulation system, portability, and flexibility in design [37–39]. The liquid flow behavior in microfluidic devices is usually laminar (or smooth and orderly). The steady laminar flow of liquid can be readily controlled, thus biomolecule transportation in the liquid can be regulated in the predictable manner [40]. Regarding to the microfluidic dimension of 1500 × 3000 × 50 μm in width × length × depth that has been used in this study, the ratio of initial force to viscose force (Reynolds number) within the liquid inside is equal to 4.605 and the constant pressure at outlet. Because the Reynolds number of the liquid flow inside this microfluidic chip is much less than 2000, the HEK cells suspended inside this microfluidic chip is supposed to be affected by laminar flow [40,41]. Based on the laminar flow effect, the HEK cells suspended in the liquid layers can be uniformly spread throughout the substrate surface. Cell suspension on the substrate surface is forced by the laminar flow. Therefore, the HEK cells located in the microfluidic chip are well distributed as a single layer. In standard microplate where gravity force dominates capillary force, cell clumping can be typically found on the substrate. The cells that locate under the cell clumps are lacked of nutrients and supplementations. So, the cell clumps cannot firmly attach on the substrate of the microplate and can be easily peeled off during IF staining process. Cell overlapping also lead to the variation of the IF signals analysis. Because LOD of the platform has been calculated by the summation of an average MFI of blank sample and standard variation of signal measured from the low concentration of analyst multiplied by 1.645. Therefore, the platform that offers the lower signal of blank and lower standard variation can give better LOD for the IgG determination. In micro-scale chamber, MOG-IgG molecules in the sample solutions are forced to incubate closer (in micrometer range) to the target cells. Therefore, incubation period of the IF assay operating in microfluidic can be greatly reduced.

5. Conclusion

This work develops a cell-based microfluidic system for serological MOG-IgG detection. The PDMS microfluidic was modified by PLL to immobilize MOG protein expressing cell. Apart from general advantages

of the microfluidic such as the potential of the device for enabling affordable mass production, ultimate reduction of reagents and sample consuming, and allowance of automatic flow regulation, we demonstrate that laminar flow in the microfluidic can promote cell distribution and the IF staining efficacy. Cell-based IF assay preformed in the microfluidic platform can improve LOD and can reduce turnaround time of the IF assay for MOG-IgG detection.

Declaration of Competing Interest

The authors declare that they have no known competing financial interests or personal relationships that could have appeared to influence the work reported in this paper.

Acknowledgments

This work was supported by Thailand's National Science and Technology Development Agency (NSTDA) (Grant No. P-16-50098) and Faculty of Medicine, Siriraj Hospital (Grant No. r015936004). The first author, Numfon Khemthongcharoen, was supported by a joint grant from the Thailand Research Fund (TRF) and Thailand's National Science and Technology Development Agency (NSTDA) under the Royal Golden Jubilee Ph.D. (RGJ-PHD) Program (Grant No. PHD/0213/2557). We would like to sincerely thank you for the facilites and the support for the fabrication of the microfluidic chips provided by TMEC.

Appendix A. Supplementary data

Supplementary data to this article can be found online at https://doi.org/10.1016/j.sbsr.2021.100458.

References

[1] G.R. Dos Passos, L.M. Oliveira, B.K. Da Costa, S.L. Apostolos-Pereira, D. Callegaro, K. Fujihara, et al., MOG-IgG-[a]ssociated optic neuritis, encephalitis, and myelitis: lessons learned from neuromyelitis optica spectrum disorder, Front. Neurol. 9 (2018) 217.
[2] P. Peschl, M. Bradl, R. Hoftberger, T. Berger, M. Reindl, Myelin oligodendrocyte glycoprotein: deciphering a target in inflammatory demyelinating diseases, Front. Immunol. 8 (2017) 529. Vol. 8, no. 8, May. 2017, Art. No. 529.
[3] M.S. Weber, T. Derfuss, I. Metz, W. Brück, Defining distinct features of anti-MOG antibody associated central nervous system demyelination, Ther. Adv. Neurol. Disord. 11 (2018) 1–5.
[4] S.L. Patterson, S.E. Goglin, Neuromyelitis Optica, Rheum. Dis. Clin. N. Am. 43 (4) (2017) 578–591.
[5] D.M. Wingerchuk, Neuromyelitis optica, Int. MS J. 13 (2) (2006) 42–50.
[6] M. Bouzar, S. Daoudi, S. Hattab, A.A. Bouzar, K. Deiva, B. Wildemann, et al., Neuromyelitis optica spectrum disorders with antibodies to myelin oligodendrocyte glycoprotein or aquaporin-4: [c]linical and paraclinical characteristics in Algerian patients, J. Neurol. Sci. 281 (2017) 240–244.
[7] D.K. Sato, D. Callegaro, M.A. Lana-Peixoto, P.J. Waters, F.M.H. Jorge, T. Takahashi, et al., Distinction between MOG antibody-positive and AQP4 antibody-positive NMO spectrum disorders, Neurology 82 (6) (2014) 474–481.
[8] J. Kitley, P. Waters, M. Woodhall, M.I. Leite, A. Murchison, J. George, et al., Neuromyelitis optica spectrum disorders with aquaporin-4 and myelin-oligodendrocyte glycoprotein antibodies: a comparative study, JAMA Neurol. 71 (3) (2014) 276–283.
[9] A. Cobo-Calvo, M. Sepulveda, R. Bernard-Valnet, A. Ruiz, D. Brassat, S. Martinez-Yelamos, et al., Antibodies to myelin oligodendrocyte glycoprotein in aquaporin 4 antibody seronegative longitudinally extensive transverse myelitis: [c]linical and prognostic implications, Mult. Scler. 22 (3) (2016) 312–319.
[10] M. Sepulveda, T. Armangue, E. Martinez-Hernandez, G. Arrambide, N. Sola-Valls, L. Sabater, et al., Clinical spectrum associated with MOG autoimmunity in adults: significance of sharing rodent MOG epitopes, J. Neurol. 263 (7) (2016), 1390–60.
[11] P. Peschl, K. Schanda, B. Zeka, K. Given, D. Bohm, K. Ruprecht, et al., Human antibodies against the myelin oligodendrocyte glycoprotein can cause complement-dependent demyelination, J. Neuroinflammation 14 (2017) 208.
[12] S. Jarius, F. Paul, O. Aktas, N. Asgari, R.C. Dale, J. De Seze, et al., MOG encephalomyelitis: international recommendations on diagnosis and antibody testing, J. Neuroinflammation 15 (1) (2018) 134.
[13] J. Kuhle, R.L. Lindberg, A. Regeniter, M. Mehling, F. Hoffmann, M. Reindl, et al., Antimyelin antibodies in clinically isolated syndromes correlate with inflammation in MRI and CSF, J. Neurol. 254 (2) (2007) 160–168.
[14] O. Connor KC, McLaughlin KA, P.L. De Jager, T. Chitnis, E. Bettelli, C. Xu, et al., Self-antigen tetramers discriminate between myelin autoantibodies to native or denatured protein, Nat. Med. 13 (2) (2007) 211–217.
[15] S. Jarius, K. Ruprecht, J.P. Stellmann, A. Huss, I. Ayzenberg, A. Willing, et al., MOG-IgG in primary and secondary chronic progressive multiple sclerosis: a multicenter study of 200 patients and review of the literature, J. Neuroinflammation 15 (1) (2018) 88.
[16] A. Marchionatti, M. Woodhall, P.J. Waters, D.K. Sato, Detection of MOG-IgG by cell-based assay: moving from discovery to clinical practice, Neurol. Sci. 42 (2021) 73–80.
[17] M. Reindl, P. Waters, Myelin oligodendrocyte glycoprotein antibodies in neurological disease, Nat. Rev. Neurol. 15 (2) (2019) 89–102.
[18] M. Reindl, K. Schanda, M. Woodhall, F. Tea, S. Ramanathan, J. Sagen, et al., International multicenter examination of MOG antibody assays, Neurol. Neuroimmunol. Neuroinflamm. 7 (2) (2020), e674.
[19] U. Brehm, S.J. Piddlesden, M.V. Gardinier, C. Linington, Epitope specificity of demyelinating monoclonal autoantibodies directed against the human myelin oligodendrocyte glycoprotein (MOG), J. Neuroimmunol. 97 (1–2) (1999) 9–15.
[20] P.J. Waters, L. Komorowski, M. Woodhall, S. Lederer, M. Majed, J. Fryer, et al., A multicenter comparison of MOG-IgG cell-based assays, Neurology 92 (11) (2019) e1250–e1251.
[21] A.S. Lopez-Chiriboga, M. Majed, J. Fryer, D. Dubey, A. McKeon, E.P. Flanagan, J. Jitprapaikulsan, et al., Association of MOG-IgG serostatus with relapse after acute disseminated encephalomyelitis and proposed diagnostic criteria for MOG-IgG-associated disorders, JAMA Neurol. 75 (11) (2018) 1355–1363.
[22] C. Poon, Measuring the density and viscosity of culture media for optimized computational fluid dynamics analysis of *in vitro* devices, bioRxiv (2020), https://doi.org/10.1101/2020.08.25.266221.
[23] R. Milo, P. Jorgensen, U. Moran, G. Weber, M. Springer, BioNumbers–the database of key numbers in molecular and cell biology, Nucleic Acids Res. 38 (2010) (BNID 108918):D750-D3.
[24] A. Blumlein, N. Williams, J.J. McManus, The mechanical properties of individual cell spheroids, Sci. Rep. 7 (1) (2017) 7346.25.
[25] L. Ho, C.L. Greene, A.W. Schmidt, L.H. Huang, Cultivation of HEK 293 cell line and production of a member of the superfamily of G-protein coupled receptors for drug discovery applications using a highly efficient novel bioreactor, Cytotechnology 45 (3) (2004) 117–123.
[26] T. Thienthong, E. Juntasaro, N. Khemthongcharoen, W. Sripumkhai, N. Houngkamhang, P. Pattamang, et al., Mixing-performance evaluation of a multiple dilution microfluidic chip for a human serum dilution process, Engl. J. 25 (9) (2021) 67–87.
[27] M.D. Abramoff, P.J. Magalhaes, S.J. Ram, Image [P]rocessing with ImageJ, Biophoton. Int. 11 (7) (2004) 36–42.
[28] D.A. Armbruster, T. Pry, Limit of blank, limit of detection and limit of quantitation, Clin. Biochem. Rev. 29 (Suppl1) (2008) S49–S52.
[29] J.C. McDonald, G.M. Whitesides, Poly(dimethylsiloxane) as a material for fabricating microfluidic devices, Acc. Chem. Res. 35 (7) (2002) 491–499.
[30] H. Zhang, M. Chiao, Anti-fouling [c]oatings of [P]oly(dimethylsiloxane) [d]evices for biological and [b]iomedical [a]pplications, J. Med. Biol. Eng. 35 (2) (2015) 143–155.
[31] A. Gokaltun, M.L. Yarmush, A. Asatekin, O.B. Usta, Recent advances in nonbiofouling PDMS surface modification strategies applicable to microfluidic technology, Technology (Singap. World Sci.) 5 (1) (2017) 1–15.
[32] S. Kuddannaya, J. Bao, Y. Zhang, Enhanced in vitro biocompatibility of chemically modified poly(dimethylsiloxane) surfaces for stable adhesion and long-term investigation of brain cerebral cortex cells, ACS Appl. Mater. Interfaces 7 (45) (2015) 25529–25538.
[33] A. Zuchowska, P. Kwiatkowski, E. Jastrzebska, M. Chudy, A. Dybko, Z. Brzozka, Adhesion of MRC-5 and A549 cells on poly(dimethylsiloxane) surface modified by proteins, Electrophoresis 37 (3) (2016) 536–544.
[34] V.A. Liu, W.E. Jastromb, S.N. Bhatia, Engineering protein and cell adhesivity using PEO-terminated triblock polymers, J. Biomed. Mater. Res. 60 (1) (2002) 126–134.
[35] L. Yu, C.M. Li, Q. Zhou, J.H.T. Luong, Poly(vinyl alcohol) functionalized poly (dimethylsiloxane) solid surface for immunoassay, Bioconjug. Chem. 18 (2) (2007) 281–284.
[36] N. Khemthongcharoen, P. Uawithya, M. Chanasakulniyom, M. Yasawong, W. Jeamsaksiri, W. Sripumkhai, et al., Polydimethylsiloxane (PDMS) microfluidic modifications for cell-based immunofluorescence assay, J. Adhes. Sci. Technol. 35 (9) (2021) 955–972.
[37] A. Burklund, A. Tadimety, Y. Nie, N. Hao, J.X.J. Zhang, Chapter One - Advances in diagnostic microfluidics, in: G.S. Makowski (Ed.), Advances in Clinical Chemistry 95, Elsevier, 2020, pp. 1–72.
[38] Y. Yang, Y. Chen, H. Tang, N. Zong, X. Jiang, Microfluidics for biomedical analysis, Small Methods 4 (4) (2020) 1900451.
[39] Q. Zhong, H. Ding, B. Gao, Z. He, Z. Gu, Advances of microfluidics in biomedical engineering, Adv. Mater. Technol. 4 (6) (2019) 1800663.
[40] J.P. Brody, P. Yager, R.E. Goldstein, R.H. Austin, Biotechnology at low Reynolds numbers, Biophys. J. 71 (6) (1996) 3430–3441.
[41] Menon E. Shashi, Chapter [f]ive - [f]luid [f]low in [P]ipes, in: E. Shashi Menon (Ed.), Transmission Pipeline Calculations and Simulations Manual, Gulf Professional Publishing, Boston, 2015, pp. 149–234.